Effect of pH and gel electrolyte on safe charge injection and electrode degradation of platinum electrodes

Thomas Niederhoffer
Department of Medical Physics and Biomedical Engineering
University College London
London, UK
thomas.niederhoffer.19@ucl.ac.uk

Anne Vanhoestenberghe
School of Biomedical Engineering and Imaging Sciences
King's College London
London, UK
a.vanhoest@kcl.ac.uk

Henry T. Lancashire
Department of Medical Physics and Biomedical Engineering
University College London
London, UK
h.lancashire@ucl.ac.uk

***Abstract*—Platinum (Pt) is a widespread electrode material choice for neural interfaces and electrochemical biosensors, due to its supposed electrochemical inertness. However, faradaic reactions can take place at Pt electrodes, including Pt oxide formation and reduction. Repeated redox cycles of Pt can lead to Pt dissolution, which may harm the tissue and significantly reduce electrode lifetime. In this study, we investigated how the electrolyte may influence Pt dissolution mechanisms during current pulsing. Two electrolyte characteristics were considered: pH and gelation. We confirmed that empirically reported tissue damage thresholds correlate with Pt oxide formation and reduction. Varying electrolyte pH occasioned a shift in recorded potentials, however, damage thresholds correlated with the same mechanisms for all pH values. The similar behaviour observed for pH values in the central range (4 ≤ pH ≤ 10) can be explained by variations of local pH at the electrode surface. Gel electrolytes behaved comparably to solutions, which was confirmed by statistical similarity tests. This study extends the knowledge about platinum electrochemistry and shows the necessity to carefully choose the stimulation protocol and the electrolyte to avoid platinum dissolution and tissue damage.**

Keywords—platinum dissolution, damage mechanisms, charge injection mechanisms, pH electrochemistry, gel electrolyte

I. Introduction

Both neural interfaces and electrochemical biosensors require charge transfer at working electrode surfaces. Increasing focus on implantable devices means that devices must be miniaturized and must function in the body environment. However, current benchtop tests overestimate safe charge injection limits in the body by 2- to 10-fold [1, 2], and were developed for electrodes with up to 1000-fold greater diameter than modern miniaturised devices [3-5]. Safe limits for galvanostatically controlled charge injection at Pt electrodes have been linked to Pt dissolution driven by platinum oxide (PtO) formation and reduction [6], placing a lower limit on safety than the typical background limits of the water window. In particular, the empirically derived Shannon's limit (eq. (1)) for current pulse safety linking charge per phase Q, charge density per phase D, and material-dependent damage limit k, is associated with PtO formation [6, 7]. Exceeding this limit during current-controlled pulsing with any electrode risks degrading sensor performance and lifetime as well as releasing toxic dissolution products.

$$log\ (D) = k + log\ (Q) \quad (1)$$

Kumsa et al. [6] developed a framework to study the underlying mechanisms of Shannon's limit by recording the electrode potential as a function of k, during biphasic current-controlled pulsing, voluntarily exceeding the damage limit to observe damage-related changes. Differences in safe limits in vivo have been attributed to differences in the electrode environment [8]. In this work we use a similar framework to Kumsa et al. [6] to investigate the effect of two characteristics of the body tissue on Pt electrode damage mechanisms: first, pH which varies with sensor location and foreign body response to implantation and stimulation [9, 10], and second, the extracellular matrix which we model as a gel electrolyte [11].

II. Material and Methods

A. Electrolytes

Unbuffered saline solutions were prepared at a range of pH by mixing a sodium chloride (NaCl) saline solution with hydrochloric acid (HCl) or sodium hydroxide (NaOH). Medical grade NaCl (MW: 58.45 $g.mol^{-1}$, Promega) was diluted in deionized water (DW, 15.6 $M\Omega.cm^{-1}$, Millipure system) at a concentration of 18 g/L or twice the isotonic concentration (0.9% w/v, equivalent to 9 g/L). HCl (1 M, Sigma-Aldrich) and NaOH (crystals, BDH) were diluted at the desired concentration in DW and mixed in a 1:1 ratio with 18 g/L NaCl to give an isotonic solution of desired pH.

Agar powder was added (0.5 wt%) to the base electrolytes, and gelation was achieved by heating to boiling point followed by cooling to room temperature. pH was adjusted following gelation. Agar gel electrolytes were prepared with three base solution electrolytes: phosphate-buffered saline (PBS), sulfuric acid (H_2SO_4) and pH 11 saline (NaOH in isotonic 0.9 wt% saline (NaCl)).

B. Electrochemical setup

A three-electrode setup composed of a Pt disk working electrode (WE, Ø 5mm), a carbon rod counter electrode (CE), and a Ag|AgCl reference electrode (RE) was used for all experiments.

A custom stimulator was designed to deliver trains of 1000 biphasic cathodic-first asymmetric pulses with a capacitive charge-balancing anodic phase, similar to cyclic chronopotentiometry, after Hudak [12]. A capacitor placed in series with the electrodes charged during the cathodic phase and reversed the charge injection during the anodic phase to ensure charge balance. WE potential excursions vs RE were measured for the 1st and 1000th pulses using a differential probe (Pico). k (see definition eq. (1)) was varied between 0.5 and 2, crossing the empirically observed damage limit for Pt at $k \approx 1.75$.

Between pulsing trains, electrodes were connected to a potentiostat (Gamry Reference 600+) to carry out a series of electrochemical tests, that would also serve as electrode conditioning sequence. Tests included electrochemical impedance spectroscopy (EIS), cyclic voltammetry (CV), and open-circuit potential (OCP) measurements. EIS was conducted between 1 Hz and 10^5 Hz centred at OCP with a 5 mV RMS amplitude. CV was conducted at a sweep rate of 100 $mV.s^{-1}$ between potentials delimitating the water window, which would vary for each electrolyte.

C. *Data analysis*

Data were analysed using custom MATLAB scripts. The potentials of interest in pulsing experiments were the start and end potential of the pulse train, the maximum anodic electrode polarization, and the maximum cathodic electrode polarization. Polarization potentials were obtained by subtracting the electrolyte ohmic drop in the cathodic and anodic phases.

To compare potential excursions in gels and solutions, statistical similarity tests were performed using MATLAB: two sample Kolmogorov-Smirnov (K-S) test and direct linear regression (DLR) comparison. K-S test was run using a built-in MATLAB function with a 95% confidence interval. DLRs comprised plotting potentials obtained for gels vs potentials for solutions (all electrolytes, all *k*-values). A linear fit was realized, and 95% confidence intervals were calculated.

III. Results

A. *Effect of pH*

Maximum anodic potential (MAP) was positive for all electrolytes and correlated with *k* (Fig 1 D). MAP would increase slowly with *k* at low *k*-values and two trends were observed when approaching the limit $k = 1.75$: for pH 1, the potential increase was less steep, showing the start of a plateau, and for pH 4, 6 and 10, the potential plateaued before increasing steeply for the largest *k*-values, when $k > 1.75$. For pH 4 and 10, the plateau at $k = 1.75$ was preceded by an inflexion in the trend of MAP with *k*. pH 12 showed an initial increase in MAP with *k*, however, then MAP was constant for all $k > 1.25$.

Minimum cathodic potential (MCP) showed similar trends to MAP (Fig 1 C). MCP correlated negatively with *k*, which was expected since increasing *k* equates to increasing the stimulation current (i is proportional to $10^{k/2}$). For all pH, MCP decreased slowly at the lowest *k*-values and decreased more steeply after. For all pH, the decrease slowed down, plateaued, or underwent an inflexion around the *k*-value limit, either before (pH 4, 6 and 10) or after (pH 1 and 12) $k = 1.75$. MCP further decreased after $k = 1.75$ for pH 4, 6 and 10.

To analyse the implications of variations in MAP and MCP, a cyclic voltammogram was aligned with the potential evolution plots (Fig 1 A & B). Projecting MAP and MCP onto CV scans shows that MAP was located in the oxide formation region for every *k*-value, and MCP was located inside or just before the Pt oxide reduction peak. For most pH values, the limit *k*-value $k = 1.75$ coincides with entering the Pt oxide reduction region during cathodic charge injection.

Similarities for pH 4, 6 and 10 were corroborated by EIS and CV measurements. Saline solutions from pH 4 to 12 had very similar impedance Bode plots, with only some discrepancy at high frequencies (f > 10 kHz) and a slightly lower impedance at high frequency for pH 12. pH 1 was substantially different, showing a 2- to 3-fold lower high frequency impedance and transition to capacitive behavior at higher frequency, by about one order of magnitude.

pH 1 and 12 had narrower water windows than pH 4, 6 and 10, which exhibited almost identical voltammograms. pH 1 was shifted towards higher potential as expected, and the voltammogram showed differences in the H-evolution region, exhibiting a larger area and peaks closer to one another, and an oxide reduction peak split into two distinct peaks. For pH 12, and slightly less for pH 10, 6 and 4, H-peaks were more spaced due to lower H^+ ion concentrations and higher overpotentials.

B. *Effect of gelation*

Three electrolytes of different pH and ionic composition (H2SO4, PBS, pH 11 saline) were formed into gel electrolytes with 0.5% agar, and the electrode response to the current-controlled pulses was compared between gels and solutions. Gels and solution had very similar anodic and cathodic potential excursions, both in trend of potential with *k*, and in absolute value. Fig 2 shows the evolution of MAP, MCP and end potential with Shannon's parameter *k*, for PBS solution and gel. As observed previously for saline solutions, MAP was positively correlated with *k*, MCP was negatively correlated with *k*, and both potentials had an inflection around Shannon's limit $k = 1.75$. Similar trends were observed for H2SO4 and pH 11 saline. The intended pH 11 saline pH varied with time, decreasing of 1 to 2 pH units over 24h, before stabilizing. Therefore, most data points were taken after stabilization at pH ≈ 10, but the similarity between gel and solution was still observed.

To quantify the similarity of potential evolution in gel and solution, three statistical comparisons were performed: Bland-Altman plot, Kolmogorov-Smirnov test (table I), and direct linear regression (DLR) plot (Fig 3).

K-S rejected the hypothesis that MAP and MCP of gels and solutions belong to different distributions, i.e. gels' and solutions' behaviours were not statistically significantly different (table I), however, noticeably different trends were observed in the DLR plots.

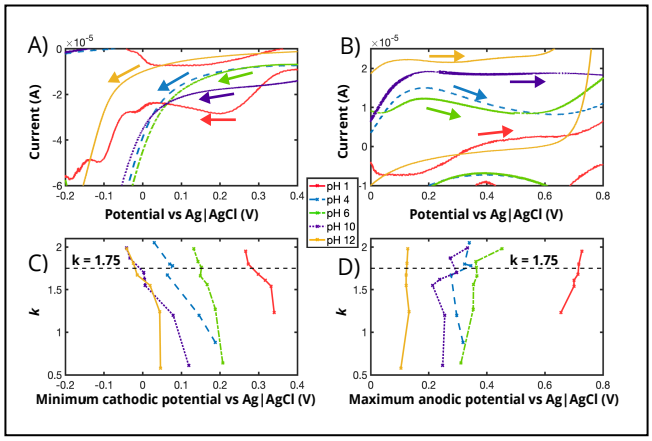

Fig. 1. Extreme potentials reached during the cathodic (D) and anodic (C) phases for each k value after 1000 biphasic cathodic-first current-controlled pulses. Above, cyclic voltammograms (A & B) were aligned to identify corresponding reactions. Arrows indicate the sweep direction.

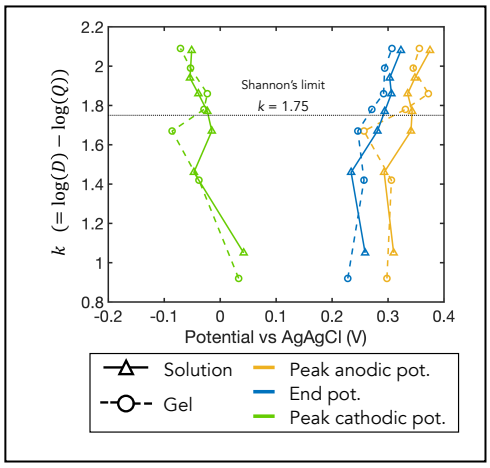

Fig. 2. Evolution of potentials of interest with Shannon's parameter k for PBS solution vs gel after 1000 biphasic cathodic-first current-controlled pulses.

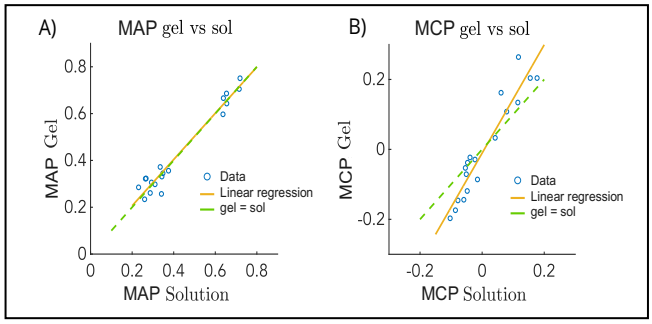

Fig. 3. Direct linear regression (DLR) plots comparing the maximum anodic potential (MAP, A) and minimum cathodic potential (MCP, B) of gel versus solution for all electrolytes, for all k values.

TABLE I. RESULTS OF TWO SAMPLE K-S TEST

K-S test results	Two sample K-S test parameters		
	Hypothesis (similarity) rejected	α [a]	***p***
MAP	0 (False)	0.95	0.99
MCP	0 (False)	0.95	0.50

[a] Confidence interval.

The DLR show very similar behaviour for MAP (Fig 3 A) between gel and solution, with the linear regression almost superimposed on the identity line (gel = solution). However, MCP (Fig 3 B) showed a visible discrepancy, with a steeper linear regression, which suggests there is a combined effect of pH and gelation. High pH electrolytes gels had consistently lower MCP than solutions, while for low pH, gels had consistently higher MCP.

IV. DISCUSSION

A. *Analysis of polarization potentials at a range of pH*

Plateaus observed for a range of pH signify that the increasing charge injection demanded by a higher stimulation intensity is not supplied by a capacitive mechanism, as this would result in a potential increase/decrease (Q=CV). Therefore, a plateau indicates that a faradaic reaction is occurring and serves as charge injection mechanism. Steep increases/decreases of potential with k indicate capacitive charge injection until the potential enters a region where faradaic reactions are able to support the required charge injection. MAP was systematically found in the oxide formation region and MCP just before or in the oxide reduction. Therefore, the plateaus observed at and above the limit k-value indicate that a faradaic reaction supplies the charge injected and it corresponds to oxide formation and reduction. For pH 1 and 12 particularly, the MAP plateau is less marked around the limit k-value, but it is clearly visible for the MCP. Moreover, the MAP was consistently found in the oxide formation region, even for low k-values, whereas MCP entered the oxide reduction region at higher k-values, around k = 1.75. Therefore, we hypothesise that the Shannon damage limit for Pt during current-controlled pulsing is linked to oxide reduction mechanisms, rather than oxide formation and is independent of pH.

The absence of pH shift for pH 4, 6 and 10 observed in CV is counter-intuitive but has also already been observed in fundamental electrochemistry. Strbac [13] found that diffusion limited currents were different for pH < 3.5 and pH > 10 but no difference was observed in between. In low buffer concentrations, outside of extreme solution pH, the local pH at the electrode surface converges to a stable value, without changing the global solution pH [13]. Therefore, even if the solution pH is measured across a range of values, the local pH will converge to a stable value, different from solution pH and the electrode behaviour will remain unchanged. Since body pH belongs to this central range (3.5 < pH < 10), it is possible that such local pH swings happen at the electrode-electrolyte interface during stimulation.

B. *Influence of gelation*

The initial hypothesis considered for gels, was that having a hydrogel electrolyte structure could reduce ionic mass transport and diffusion coefficients and change the electrode polarization. Additionally, there is evidence that proteins may adsorb on the electrode surface, thereby influencing polarisation at the interface [14]. While similar behaviours were observed on individual electrolytes between gels and solutions, the comparison of three electrolytes of different pHs unveiled a noticeable trend. A combined effect of gel and pH on cathodic polarization was shown, whereas no effect on anodic polarization appeared. This means that the gelation affects the reaction(s) involved in cathodic charge injection, possibly PtO reduction, without affecting anodic charge injection reactions. Future work will consider higher gel concentrations and alternative cellular tissue models.

V. CONCLUSION

The aim of this study was to characterize the effects of pH and gel structure on the safe charge injection limit of Pt electrodes. Despite showing a clear potential shift, pH did not influence damage mechanisms, which were linked to Pt dissolution during PtO reduction. Gel electrolytes modelling the extracellular matrix structure did not statistically significantly influence charge injection, however, a noticeable discrepancy was observed on cathodic polarization only, which suggests gelation affects cathodic charge injection mechanisms, including PtO reduction, but not anodic charge injection mechanisms. This must be considered for neural interfaces and electrochemical biosensors using cyclic chronopotentiometry which may repeatedly cross the Pt oxidation/reduction potential boundary.

REFERENCES

[1] R. T. Leung, M. N. Shivdasani, D. A. Nayagam, R. K. Shepherd, "In vivo and in vitro comparison of the charge injection capacity of platinum macroelectrodes.", *IEEE Transanctions on Biomedical Engineering*, vol. 62, no. 3, pp 849-857, March 2015, doi: 10.1109/TBME.2014.2366514

[2] S. F. Cogan, K. A. Ludwig, C. G. Welle, P. Takmakov, "Tissue damage thresholds during therapeutic electrical stimulation.", *Journal of Neural Engineering*, vol. 13, no. 2, pp 021001, January 2016, doi: 10.1088/1741-2560/13/2/021001

[3] S. B. Brummer, M. J. Turner, "Electrochemical considerations for safe electrical stimulation of the nervous system with platinum electrodes.", *IEEE Transactions on Biomedical Engineering*, vol. 24, no. 1, pp 59-63, January 1977, doi: 10.1109/TBME.1977.326218

[4] D. B. McCreery, T. G. H. Yuen, W. F. Agnew, L. A. Bullara, "Stimulus parameters affecting tissue injury during microstimulation in the cochlear nucleus of the cat". *Hearing research*, vol. 77, no. 1-2, pp 105-115, June 1994, doi: 10.1016/0378-5955(94)90258-5

[5] D. R. Merrill, M. Bikson, J. G. Jefferys, "Electrical stimulation of excitable tissue: design of efficacious and safe protocols.", *Journal of Neuroscience Methods*, vol. 141, no. 2, pp 171-198, February 2005, doi: 10.1016/j.jneumeth.2004.10.020

[6] D. W. Kumsa, F. W. Montague, E. M. Hudak, J. T. Mortimer, "Electron transfer processes occurring on platinum neural stimulating electrodes: pulsing experiments for cathodic-first/charge-balanced/biphasic pulses for $0.566 \leq k \geq 2.3$ in oxygenated and deoxygenated sulfuric acid.", *Journal of Neural Engineering*, vol. 13, no. 5, pp 056001, July 2016, doi: 10.1088/1741-2560/13/5/056001

[7] R. V. Shannon, "A model of safe levels for electrical stimulation." *IEEE Transactions on Biomedical Engineering*, vol. 39, no. 4, pp 424-426, April 1992, doi: 10.1109/10.126616

[8] A. R. Harris, P. Carter, R. Cowan, G. G. Wallace, "The Impact of Protein Fouling on the Charge Injection Capacity, Impedance and Effective Electrode Area of Platinum Electrodes for Bionic Devices », *ChemElectroChem*, vol. 8, no. 6, pp 1078-1090, February 2021, doi: 10.1002/celc.202001574

[9] O. Korostynska, K. Arshak, E. Gill, A. Arshak, "Review Paper: Materials and Techniques for In Vivo pH Monitoring", *IEEE Sensors Journal*, vol. 8, no. 1, pp 20-28, December 2007, doi: 10.1109/JSEN.2007.912522

[10] C. Q. Huang, P. M. Carter, R. K. Shepherd, "Stimulus Induced pH Changes in Cochlear Implants: An In Vitro and In Vivo Study", *Annals of Biomedical Engineering*, vol. 29, no. 9, pp 791-802, 2001, doi: 10.1114/1.1397793

[11] S. M. O'Connor, D. A. Stenger, K. M. Shaffer, W. Ma, "Survival and neurite outgrowth of rat cortical neurons in three-dimensional agarose and collagen gel matrices." Neuroscience Letters, vol. 304, no. 3, pp 189-193, May 2001, doi: 10.1016/S0304-3940(01)01769-4

[12] E. M. Hudak, "Electrochemical evaluation of platinum and diamond electrodes for neural stimulation" (Doctoral dissertation, Case Western Reserve University), 2011, OhioLINK Electronic Theses and Dissertations Center. http://rave.ohiolink.edu/etdc/view?acc_num=case1301967862

[13] S. Strbac, "The effect of pH on oxygen and hydrogen peroxide reduction on polycrystalline Pt electrode.", *Electrochimica Acta*, vol. 56, no. 3, pp 1597-1604, January 2011, doi: 10.1016/j.electacta.2010.10.057

[14] A. Carnacer-Lombarte, H. Lancashire, A. Vanhoestenberghe, "*In vitro* biocompatibility and electrical stability of thick-film platinum/gold alloy electrodes printed on alumina", *Journal of Neural Engineering*, vol. 14, no. 3, pp 036012, March 2017, doi: 10.1088/1741-2552/aa6557